Environmental Science & Technology

Article

pubs.acs.org/est

Heterogeneous OH Oxidation of Motor Oil Particles Causes Selective Depletion of Branched and Less Cyclic Hydrocarbons

Gabriel Isaacman,[†,*] Arthur W. H. Chan,[†] Theodora Nah,[‡] David R. Worton,[†,§] Chris R. Ruehl,[∥] Kevin R. Wilson,[∥] and Allen H. Goldstein[†,⊥,#]

[†]Environmental Science, Policy, and Management, University of California, Berkeley, California, United States

[‡]Chemistry, University of California, Berkeley, California, United States

[§]Aerosol Dynamics Inc., Berkeley, California, United States

[∥]Chemical Sciences Division, Lawrence Berkeley National Laboratory, Berkeley, California, United States

[⊥]Environmental and Energy Technologies Division, Lawrence Berkeley National Laboratory, Berkeley, California, United States

[#]Civil and Environmental Engineering, University of California, Berkeley, California, United States

Supporting Information

ABSTRACT: Motor oil serves as a useful model system for atmospheric oxidation of hydrocarbon mixtures typical of anthropogenic atmospheric particulate matter, but its complexity often prevents comprehensive chemical speciation. In this work we fully characterize this formerly "unresolved complex mixture" at the molecular level using recently developed soft ionization gas chromatography techniques. Nucleated motor oil particles are oxidized in a flow tube reactor to investigate the relative reaction rates of observed hydrocarbon classes: alkanes, cycloalkanes, bicycloalkanes, tricycloalkanes, and steranes. Oxidation of hydrocarbons in a complex aerosol is found to be efficient, with approximately three-quarters (0.72 ± 0.06) of OH collisions yielding a reaction. Reaction rates of individual hydrocarbons are structurally dependent: compared to normal alkanes, reaction rates increased by 20−50% with branching, while rates decreased ∼20% per nonaromatic ring present. These differences in rates are expected to alter particle composition as a function of oxidation, with depletion of branched and enrichment of cyclic hydrocarbons. Due to this expected shift toward ring-opening reactions heterogeneous oxidation of the unreacted hydrocarbon mixture is less likely to proceed through fragmentation pathways in more oxidized particles. Based on the observed oxidation-induced changes in composition, isomer-resolved analysis has potential utility for determining the photochemical age of atmospheric particulate matter with respect to heterogeneous oxidation.

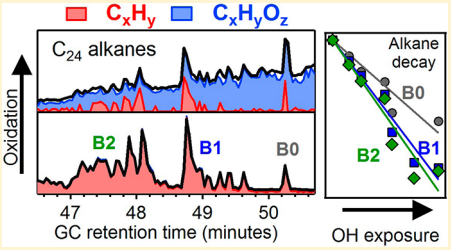

1. INTRODUCTION

In urban regions, a significant fraction of submicrometer organic particulate matter is comprised of chemically reduced hydrocarbons.[1] Atmospheric oxidation of these particulate hydrocarbons, primarily by the hydroxyl radical (OH), results in a prevalence of oxygenated aerosols, especially in rural and remote regions. Oxidation of particles is an efficient process, with 25% to 100% of OH-particle collisions resulting in reaction,[2−10] but significant uncertainty still remains regarding the various atmospheric oxidation pathways. This oxidation can result in the addition of oxygenated functional groups (functionalization), resulting in lower volatility products, or decomposition into higher volatility products (fragmentation). The balance between these mechanisms is influenced by compound structure,[2] with some evidence that functionalization and fragmentation depend on branching and cyclization. An improved understanding of particle phase oxidation is therefore necessary for accurate source apportionment and modeling the quantity and chemical properties of atmospheric aerosol.

Heterogeneous oxidation processes are typically considered in terms of an oxidant uptake coefficient, γ. Measured as the reactive decay of a species upon exposure to an oxidant such as the hydroxyl radical (OH), γ describes the fraction of OH collisions with a compound that result in a reaction.[3] However, OH uptake by compounds in a particle is a complex process, influenced by thermodynamic phase, diffusion, particle size and a host of physical parameters, hindering universally applicable parametrization of these processes. In multicomponent systems, focusing on relative relationships between rates or OH uptake coefficients of different species reduces uncertainty from physical parameters, providing broader understanding of the oxidation processing of various compounds and theoretically extending utility to other oxidative environments.[11]

OH uptake of compounds is dependent on particle composition,[12] so heterogeneous oxidation of hydrocarbons

Received: July 9, 2012
Revised: August 31, 2012
Accepted: September 4, 2012
Published: September 4, 2012

dx.doi.org/10.1021/es302768a | Environ. Sci. Technol. 2012, 46, 10632−10640

within a motor oil particle[6,13,14] provides a more realistic surrogate system for the atmospheric processing of anthropogenic aerosols than single-component particles. However, these hydrocarbon mixtures are comprised of hundreds to thousands of compounds,[15] most of which are unresolvable using traditional techniques, so past work has generally focused on a small fraction of the chemicals in diesel fuel and motor oil that are resolvable and can serve as molecular markers for these sources. This work provides a more comprehensive analysis of heterogeneous oxidation of these hydrocarbon mixtures by combining gas chromatography with soft photoionization mass spectrometry.

Traditional gas chromatography and mass spectrometry (GC/MS) relies on 70 eV electron impact (EI) ionization. Most organic compounds have an ionization energy below 11 eV,[16] so the excess energy provided by these electrons results in a mass spectrum populated by small fragment ions that are nearly indistinguishable for structurally similar compounds. "Unresolved complex mixtures" containing compounds that cannot be separated chromatographically or through EI mass spectra can be better resolved by "soft ionization" GC techniques that minimize fragmentation, thus preserving the molecular ion for identification. This vastly improves resolution of structural isomers through separation by ion mass-to-charge ratio (m/Q).

Soft ionization is achieved in this work by using vacuum-ultraviolet (VUV) photons generated by synchrotron radiation as an ionization source.[17] Though a variety of other methods of photon generation are available,[18−20] synchrotrons provide the flexibility of adjusting photon energy between 8 and 11 eV, with a reliable and relatively high photon flux.[21] The separation and resolution capabilities of VUV-MS are unparalleled when coupled to a gas chromatograph[22,23] for characterizing unknown compounds by carbon number, number of double bonds and rings, and degree of branching,[17] providing a nearly comprehensive compositional analysis of unresolved complex hydrocarbon mixtures.

In this work we apply the separation capabilities of GC/VUV-MS to measure the OH oxidation rates of hydrocarbons in motor oil particles. Comprehensive characterization of the hydrocarbon mixture is accomplished using high resolution (HR) mass spectrometry to separate oxygenated and non-oxygenated peaks in the mass spectrum in order to quantify oxidative decay of each compound class observed in motor oil: alkanes, cycloalkanes, bicycloalkanes, tricycloalkanes, and steranes. Relative reaction rates of resolved individual hydrocarbon classes and structural isomers are reported and combined with compositional analysis to determine the average OH uptake coefficient for total unreacted hydrocarbons. Implications of differences in relative rates are discussed in the context of modeling oxidation of urban organic aerosol, as the composition and fates of particulate hydrocarbons are expected to change with time.

2. EXPERIMENTAL SECTION

2.1. Flow Tube Reactor. The flow tube reactor used in this work has been previously described in detail,[3,24] including schematic drawings of the setup. SAE 15W-40 motor oil particles were produced by homogeneous nucleation of new motor oil at 122 °C, creating polydisperse aerosol with a log-normal size distribution (mean surface-weighted diameter = ∼170 nm) and a concentration of ∼2600 $\mu g/m^3$; at this particle loading, compounds with volatilities of a C_{22} alkane and lower are expected to be more than 90% in the particle phase. Particles were entrained in nitrogen and passed through an annular charcoal denuder to the flow tube reactor (type 219 quartz, 130 cm long, 2.5 cm i.d.), in which they were exposed to hydroxyl (OH) radicals. The average residence time in the flow tube was ∼37 s. The OH radicals were generated through the photolysis of ozone (corona discharge generator, OzoneLab Instruments) by mercury lamps (λ = 254 nm) in the presence of water vapor (∼30% relative humidity). OH exposure (concentration × time) was measured by the decay of *n*-hexane introduced at the top of the flow tube for low OH concentrations. At high OH concentrations, hexane is introduced instead at the bottom of the tube to avoid depletion below the level of detection and calculation of OH exposure includes a multiplicative factor which is found through empirical calibration (uncertainty of ±5%) before data collection.[24] Error in reported OH exposures is dominated by the uncertainty in the gas-phase rate constant, which is 20−30%, though estimated to be closer to 10%.[25] While OH concentrations generated in this experimental setup were typically several orders of magnitude larger than atmospherically relevant levels, high OH concentrations have been shown to yield roughly consistent results to longer duration and lower−OH experiments.[5,26]

Hexane concentration in the outflow of the reactor was monitored by a gas chromatograph with a flame ionization detector (SRI Instruments), and particle concentration and size was measured with a scanning mobility particle sizer (TSI). Samples for speciated organic analysis were collected for 10−60 min at a flow rate of 0.2−0.6 lpm (mass flow controller, MKS Instruments) on quartz fiber filters (47 mm Tissuquartz, Pall Life Science, prebaked at 600 °C) downstream of a charcoal denuder (8 in. 480-channel MAST Carbon) to avoid gas-phase adsorption on the filters. Experiments were performed at seven different OH exposures ranging from 0 to 1.3×10^{12} molecules cm^{-3} s.

2.2. GC/VUV-HRTOFMS. Filter samples were analyzed by thermal desorption and gas chromatography coupled to high-resolution vacuum-ultraviolet time-of-flight mass spectrometry (GC/VUV-HRTOFMS). Filter punches (2−6 punches of 0.4 cm^2 each) were thermally desorbed under helium using a commercial thermal desorption system and autosampler (TDSA, Gerstel) into a gas chromatograph (Agilent 7890). A first dimension 60 m × 0.25 mm × 0.25 μm nonpolar column (Rxi-5Sil MS, Restek) was coupled to a second dimension polar column (1 m × 0.25 mm × 0.25 μm, Rtx-200MS, Restek) with a modulator (Zoex) to allow for GC × GC analysis, although second dimension data will not be presented here. Effluent from the column was analyzed using a high-resolution ($m/\Delta m \approx 4000$) time-of-flight mass spectrometer (HTOF, Tofwerk) coupled to the Chemical Dynamics Beamline (9.0.2) at the Advanced Light Source at Lawrence Berkeley National Laboratory, described in detail by Heimann et al.[21] Vacuum-ultraviolet photons were passed through an argon gas cell and a MgF_2 window to remove unwanted high frequency undulator harmonics, providing photons for these measurements of 10.5 eV with a bandwidth of 0.2 eV and a flux of $\sim 10^{15}$ photons/s.

The initial composition of motor oil (i.e., before oxidation) was quantified by structure and volatility using GC × MS analysis as described in detail by Isaacman et al.[17] Separation by retention time and m/Q allowed the determination of carbon number (N_C), cyclization (number of double bond equivalents, N_{DBE}), and degree of branching of compounds ("B0" for

straight chain, "B1" for a single branch, etc.), providing a basis for understanding the structure of the complex hydrocarbon mixture. Soft ionization provides the molecular weight of a hydrocarbon, which can be used to infer N_C, whereas N_{DBE} is determined by a difference in m/Q per ring of 2 Th (mass-to-charge, 1 Thomson = 1 Da e^{-1}). This is most accurately described as a measurement of degree of unsaturation, so the term double bond equivalents is used in this and other work, though in the case of motor oil this loss of hydrogens is expected to be due primarily to cyclization. Though resolving compounds solely by mass can be ambiguous, cyclization results in a shift in retention time as a means to distinguish isobaric compounds − for instance, naphthalene, $C_{10}H_8$, and nonane, C_9H, have the same mass but differ in retention time by several minutes (2 to 3 carbon numbers). Branching also affects retention time, such that a highly branched alkane (i.e., B4) elutes significantly earlier than a straight-chain alkane (B0) of the same carbon number, allowing separation of compounds by number of branches. Motor oil contains little unsaturated aliphatic or polycyclic aromatic mass,[27] so the hydrocarbon fraction can be grouped into classes of branched and straight-chain hydrocarbons including alkanes, cycloalkanes, bicycloalkanes, and tricycloalkanes (N_{DBE} = 0 through 3, respectively), alkylbenzenes and steranes, (N_{DBE} = 4), and tetralins and hopanes (N_{DBE} = 5).

Calibrations of GC/MS response were performed for each compound class based on a variety of relevant compounds of similar volatility and structure. These calibration response factors are expected to correct for thermal desorption efficiency (volatility dependent), GC transfer efficiency (volatility and structure dependent), and photoionization cross-section and efficiency (structure dependent). This calibration method, using structurally relevant compounds, has been shown to achieve approximately 90% mass closure in the case of diesel fuel and compare quantitatively to compounds measured by traditional methods.[28] Multipoint calibrations were performed for C_{12}−C_{28} *n*-alkanes, two branched alkanes: phytane (B4, C_{19}) and squalane (B6, C_{30}), one cycloalkane: pentadecylcyclohexane (C_{21}), C_9−C_{15} *n*-alkyl benzenes, and a mixture of polycyclic aromatic hydrocarbons, providing response factors for N_{DBE} = 0, 1, 4, and 7+. A comparison between branched and unbranched alkanes and polycyclic aromatic hydrocarbons (naphthalene, methyl naphthalene, dimethyl naphthalene, methyl biphenyl, dimethyl biphenyl, phenanthrene, pyrene, methyl pyrene) was used to determine the effects of branching on the GC/MS response of cyclic compounds. Calibration curves for these compounds are provided in SI Figure S-1 and are shown to be reasonably linear. Response factors for N_{DBE} classes without known standards were determined through interpolation of the known response factors. Authentic standards were purchased from Sigma-Aldrich, AccuStandard, and TCI.

2.3. High-Resolution Data Processing. All data processing was performed using custom code written in Igor Pro 6.22 (Wavemetrics). High-resolution data was analyzed using a technique similar to that described by DeCarlo and coworkers[29] and incorporated into the Peak Integration by Key Analysis (PIKA) software tool,[30] widely used in the atmospheric sciences for analysis of HTOF data. The spectrometric signal at a given nominal mass was deconvoluted into component peaks by minimizing the residual of a fit based on exact masses of candidate C_xH_y and $C_xH_yO_z$ peaks likely to be present. To account for deviations from Gaussian peak shapes and drifts in mass calibration, a peak shape was selected and mass calibration was performed using frequently and regularly spaced per-deuterated normal alkanes (C_{12}, C_{16}, C_{20}, C_{24}, C_{28}; C/D/N Isotopes) spiked onto the filter before desorption. Candidate peaks to be fit were selected based on the composition of unoxidized motor oil particles, which is shown in Figure 1 to not contain a significant fraction of

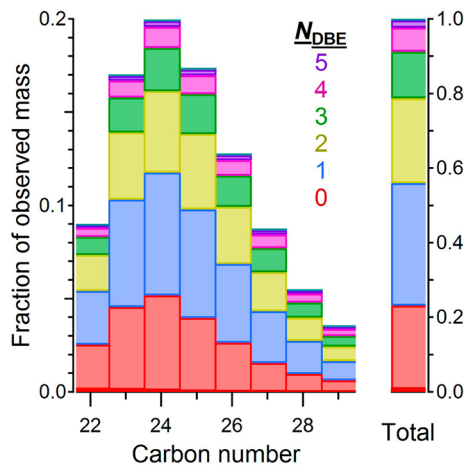

Figure 1. Contribution of each compound class to total observed mass. Except for straight-chain alkanes (shown in dark red) all mass is branched, and classes (N_{DBE}) include alkanes (0, red), cyclocalkanes (1, blue), bicycloalkanes (2, yellow), tricycloalkanes (3,green), steranes and alkylbenzenes (4, pink), and hopanes and tetralins (5, purple).

polycyclic aromatic hydrocarbons, in approximate agreement with literature motor oil composition.[27] This also conveniently avoids uncertainty from a nominal mass containing multiple potential hydrocarbons with different mass defects. Oxidized peaks were allowed to have up to four oxygen atoms, of which at most one was expected to be a hydroxyl group. These constraints reflect typical limitations of GCs, which have poor transfer efficiency for large, highly oxygenated compounds, especially hydroxyl groups (i.e., compounds presented by Williams et al.[31]). Though variations of these deconvolution parameters were explored, these constraints were found to provide a satisfactorily low residual signal and the fit was not significantly improved by allowing additional oxygen atoms.

The validity of peak deconvolution was investigated to confirm that signal was properly attributed despite the small difference in mass defect between oxygenated and non-oxygenated compounds in the carbon number range of interest. The same list of candidate peaks was used regardless of OH exposure to avoid potential biases and peak deconvolution of unoxidized motor oil particles found little oxygenated mass, confirming that hydrocarbon mass was not incorrectly identified as oxygenated. Furthermore, peak-fitting of known compounds in the volatility range of interest yields accurate molecular formulas with less than 10% of mass attributed incorrectly. The described peak-fitting method was found to yield log−linear decay of the hydrocarbon signal (R^2 > 0.7 for nearly all individual hydrocarbon classes), as well as reasonable growth of the oxygenated signal suggesting relatively accurate attribution of signal between oxygenated and nonoxygenated fractions. Most of the signal is found to contain one to three oxygen atoms, though peak-assignment in this work will be limited to oxygenated versus nonoxygenated.

2.4. Relative Rate Calculations. Uptake coefficients can be derived through the measurement of the decay of a compound, i, upon exposure to OH to yield an effective rate constant, $k_{\mathrm{eff},i}$, that is a direct measure of reaction rate, influenced by physical factors such as particle diameter and phase state:[6,11]

$$\frac{\partial \ln C_i}{\partial t} = k_{\mathrm{eff},i} C_{\mathrm{OH}} \quad (1)$$

Assuming that chromatographic signal (S_i) is a linear function of analyzed mass (supported by calibration curves shown in Figure S-1), the theoretical relationship between the concentration of OH radical (C_{OH}), the concentration of a compound (C_i), and time (t) can be expressed in an empirically useful form:

$$\ln \frac{S_{t,i}}{S_{0,i}} = k_{\mathrm{eff},i}\{C_{\mathrm{OH}} t\} \quad (2)$$

where the OH exposure, $\{C_{\mathrm{OH}}\ t\}$, is determined from the decay of the gas-phase tracer, hexane. Using eq 2, $k_{\mathrm{eff},i}$ can be calculated from the slope of the chromatographic signal of i at time t ($S_{t,i}$) relative to initial measured signal ($S_{0,i}$) (normalized for sample volume) as a function of OH exposure. To account for errors in apportioning mass by high-resolution data processing, which are poorly constrained, 1000 different values for $k_{\mathrm{eff},i}$ were calculated for each analyte of interest by varying the data points included in eq 2 (i.e., which values of $S_{t,i}$ were considered valid). Samples with the lowest hydrocarbon fractions (the most oxidized filters) were randomly included or excluded, as these samples are more likely to have points below detection limit (which was allowed to vary in this analysis), or incorrect peak deconvolution from the high-resolution analysis. In addition, the threshold for goodness of fit necessary to be considered was varied around a mean of R^2 = 0.70 (Gaussian distribution with a standard deviation of 0.10). Rates and uptake coefficients reported in this work are the averages and standard deviations of these 1000 computations.

Measured reaction rates cannot adequately be described by $k_{\mathrm{eff},i}$ as this quantity is a strong function of physical parameters such as particle surface area, density, mixing, and phase state. Therefore, the heterogeneous oxidation rate can more accurately be considered in terms of the fraction of OH collisions with a compound of interest, i, that result in the loss of the compound, given as the effective OH uptake coefficient, γ_{eff}, after Smith et al.:[3]

$$\gamma_{\mathrm{eff},i} = \frac{4 \times k_{\mathrm{eff},i} \times D_{p,\mathrm{surf}} \times \rho \times N_{\mathrm{A}}}{6 \times \bar{\tau} \times M_i} \quad (3)$$

where $D_{p,\mathrm{surf}}$ is the mean surface weighted diameter, ρ is the particle density (approximately 0.8 g cm^{-3} for a hydrocarbon mixture), N_{A} is Avogadro's number, $\bar{\tau}$ is the average speed of the OH radical, and M_i is the molecular weight of i. Measured effective reaction rate constants can include secondary radical chain chemistry or gas-phase processing,[6] yielding an effective uptake coefficient of significantly greater than 1.

In a complex system such as motor oil, the fraction of OH collisions with unreacted hydrocarbons resulting in reaction, $\gamma_{\mathrm{eff}}^{\mathrm{tot}}$, can be directly measured from the decay of total hydrocarbon mass, providing an overall rate for the transformation of unoxidized to lightly oxidized particles. The total uptake of OH by hydrocarbons in the particle must also be the sum of the relative uptake of all component compounds, assuming a well-mixed particle so that there is no preferential uptake by surface compounds. OH-hydrocarbon collisions resulting in loss of a given hydrocarbon, i, are therefore dependent on the probability of interaction with that compound, a function of the mole fraction of the compound, χ_i:

$$\gamma_{\mathrm{eff}}^{\mathrm{tot}} = \sum_i \chi_i \gamma_{\mathrm{eff},i} \quad (4)$$

Total hydrocarbon OH uptake measured through these two methods should be approximately equal in the case of internally consistent measurements.

3. RESULTS AND DISCUSSION

3.1. GC × MS Analysis. Characterization of the unresolved complex mixture in unoxidized motor oil particles (Figure 1) showed a significant contribution from alicyclic compounds with little polycyclic aromatic hydrocarbon mass, as observed in previous work.[27] While some compound classes contained a resolvable B0 isomer, such as n-alkanes and n-alkylcyclohexanes, greater than 90% of the mass in all compound classes was observed as branched isomers. The mass of the motor oil particles was centered on C_{24} compounds, a lower carbon number than in directly injected motor oil, which was observed qualitatively to have a center of mass several carbon numbers larger though was not quantified in this work. This difference is due to the relatively low temperature homogeneous nucleation of the motor oil particles, which results in particles depleted in less volatile compounds, but is not expected to affect the kinetics results presented here, which depend on the initial composition of the particles not the parent motor oil.

GC × MS analysis provides a useful tool for understanding the oxidation processes by component hydrocarbons when coupled with high-resolution peak deconvolution of mass spectra (Figure 2). The oxygenated fraction (blue signal in Figure 2) shifts toward longer GC retention time than hydrocarbons (red signal) of a given carbon number. Retention time, a proxy for volatility, of a given n-alkane (black circles in Figure 2) is similar to that of a ketone of approximately two carbon numbers smaller as would be expected based on

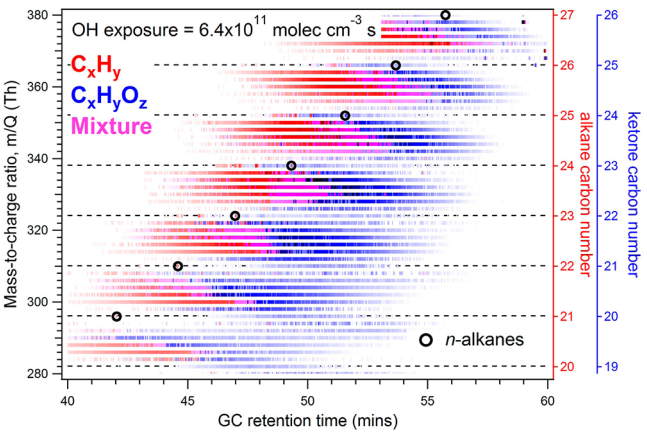

Figure 2. GC × MS plot of intermediately oxidized motor oil (6.4 × 10^{11} molecules cm^{-3} s, approximately half the exposure of the most oxidized sample). Points with a majority of the observed signal (greater than 55%) in the hydrocarbon fraction are shown in red, while majority oxygenated points are shown in blue. Points with no clear major fraction (evenly split, ± 5%) are shown in purple. The locations of normal alkanes are circled in black.

volatility calculations.[32,33] The complexity of the mixture is demonstrated by the lack of well-defined peaks in either the oxygenated or nonoxygenated fraction, but classification of these large unresolved signals by structure based on GC × MS allowed calculation of relative reaction rates for different structural classes.

The oxidation of tetracosane (C_{24}) and its lightly branched (B1 and B2) isomers provides an excellent case study of the oxidative decay of hydrocarbons, as shown in Figure 3, where

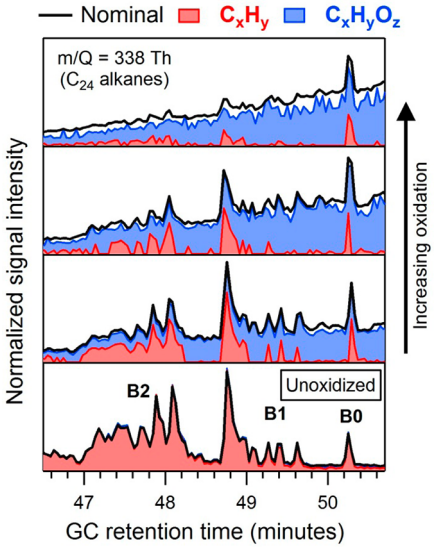

Figure 3. Oxygenated and hydrocarbon fractions of m/Q = 338 Th in the region of straight (B0) and lightly branched (B1, B2) C_{24} alkanes at four OH exposures (from bottom to top): unoxidized, 6.4×10^{11}, 7.3×10^{11}, and 1.3×10^{12} molecules cm^{-3} s^{-1}. Nominal mass signal (black line) is deconvoluted into hydrocarbon (red) and oxygenated (blue) fractions. Approximately 20% of signal is unassigned in the most oxidized panel, likely due to low signals that do not cross the background threshold for peak-fitting.

the nominal mass signal at m/Q = 338 Th is separated into oxygenated and nonoxygenated signal fractions. In unoxidized particles, all mass is contained in the hydrocarbon fraction (C_xH_y) as expected, while oxidation results in a relative increase of the oxygenated fraction ($C_xH_yO_z$). As OH exposure increases, well-resolved alkane isomer peaks are increasingly difficult to distinguish using nominal mass resolution but are extracted through high-resolution analysis. Though the shape of each isomer region remains similar, the relative intensity of each region changes. B1 and B2 isomers in this region decay at roughly the same rate, but the *n*-alkane decays much more slowly; the most abundant B1 isomers reduce from approximately 3 times the peak height of the *n*-alkane to half its height in the most oxidized sample. These observed differences in oxidation rates between isomers can be quantified using a relative rates approach.

3.2. Structurally Resolved Relative Rates of Oxidation.

Calculation of relative rates is demonstrated on C_{24} alkane isomers in Figure 4, in which the slope of the linear regression (R^2 > 0.85 for all isomers shown in Figure 4) equals the effective rate constant, $k_{eff,i}$ as described by eq 2. As was qualitatively observed in Figure 3, tetracosane (the B0 isomer) was removed at a significantly slower rate than branched isomers. Lightly branched (B1 to B3) C_{24} isomers reacted more

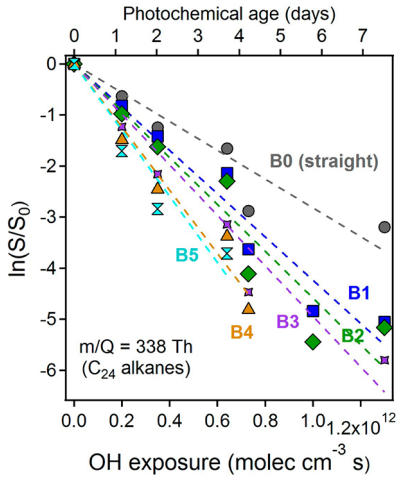

Figure 4. Relative decay of C_{24} straight (B0: gray circles) and branched alkanes (B1: blue squares, B2: green diamonds, B3: purple crosses, B4: gold triangles, B5: cyan hourglasses) as shown by logarithmic decrease of measured detector signal (S) relative to initial signal (S_0) with OH exposure. Steeper slopes indicate faster oxidation rates. Uncertainty in fits is shown by error bars in Figure 5a. Approximate photochemical age is calculated assuming an OH concentration of 2×10^6 molecules cm^{-3}.

than 50% faster than the straight chain alkane, while more branched isomers oxidized approximately twice as fast.

Effective rate constants were measured for all observed compound classes and resolved isomers and converted to effective uptake coefficients using eq 3 (Figure 5). Uptake coefficients were near or less than 1 for all compounds, while previous work conducted at atmospherically relevant particle concentrations found γ_{eff} values for compounds in this volatility range to be an order of magnitude larger than those shown in Figure 5.[6] This supports the conclusion of Lambe and co-workers that a significant amount of oxidation of these compounds in the atmosphere occurs through gas-phase processes, while confirming that due to the high particle concentrations the data presented in this work provide insight primarily into particle-phase and heterogeneous reactions. The values of γ_{eff} measured here are not descriptions of oxidation in atmospheric conditions, but rather an idealized investigation into the kinetics of the heterogeneous processes affecting these compounds. The carbon number dependence of γ_{eff} observed for all compound classes (Figure 5a,b) may be due to the presence of some gas-phase oxidation of the lighter hydrocarbons though this effect is not expected to be large because alkanes C_{23} and larger are predicted to be almost entirely in the particle phase.

While γ_{eff} is a useful means of displaying the data and making comparisons across carbon numbers and laboratory environments, discussing average relative values provides insight into effects of structure on OH uptake. Figure 5 is shown in relative terms in the Supporting Information (SI Figure S-2) to provide more detail to the interested reader beyond the average relative values and comparisons discussed below. From Figure 5a it is clear that branched isomers had faster oxidation rates than straight alkanes of the same carbon number in all cases. Across all carbon numbers, lightly branched (B1 and B2) alkanes account for a majority of the alkane mass and reacted on average 48% faster than straight alkanes, while more heavily branched isomers (B3 through B5) reacted 67% faster. Branching increases volatility, so dependence of γ_{eff} on number

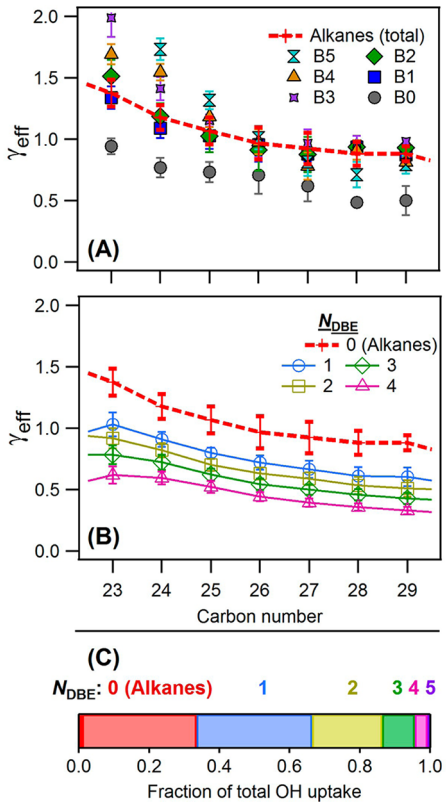

Figure 5. Effective uptake coefficients of (a) alkane isomers, and (b) cyclic compounds; the total alkane values (red dashed line) are the same in both plots. (c) Contribution of each compound class to total observed mass and total OH uptake. The measured total uptake coefficient, γ_{eff}^{tot}, equals 0.72 ± 0.06. Colors and symbols are the same used in Figures 1 and 4: classes (N_{DBE}) measured include alkanes (0, red; straight chain in darker red), cycloalkanes (1, blue), bicycloalkanes (2, yellow), tricycloalkanes (3, green), steranes and alkylbenzenes (4, pink), and hopanes and tetralins (5, purple). A majority of the mass in all compound classes is branched. Values shown are averages and standard deviations (error bars) of 1000 computations in which variables were randomly varied to gauge sensitivity to poorly constrained error.

of branches may be an artifact of gas-phase processing. Indeed, this dependence on degree of branching was not observed for higher molecular weight alkanes, which are less likely to be affected by partitioning; above C_{26}, all branched isomers reacted approximately 44 ± 14% faster than *n*-alkanes of the same carbon number.

The effects of volatility and partitioning can be accounted for using chromatographic retention time, as it is a function of vapor pressure.[33] A fit of *n*-alkane uptake coefficients with respect to retention times yields a polynomial function modeling expected γ_{eff} for theoretical *n*-alkanes of a given approximate volatility. Branched isomers of all carbon numbers were found to react 28 ± 11% faster than modeled straight chain alkanes of the same retention time, regardless of number of branches (data shown in SI Figure S-3). Based on volatility corrections and the rates of high molecular weight alkanes, we infer heterogeneous OH uptake to be 20−50% faster for all branched alkane isomers.

The reason for increased OH uptake by branched alkanes is unknown. Previously reported models predict branching to have a smaller effect on reaction rates than observed in this work. While calculations based on structure−activity relationships predict a straight chain C_{24} alkane to react less than 10% slower than branched isomers, this work suggests differences in oxidation rates are non-negligible and may be masked by uncertainties in these relationships of up to 40% for acyclic alkanes.[34]

Cyclization was also observed to affect oxidation rate. Although cyclic aliphatic compounds were expected to react with OH radicals faster than acyclic hydrocarbons[34] based on structure activity relationships, we observed the inverse (Figure 5b). Cycloalkanes reacted 27 ± 3% more slowly than *n*-alkanes, and with the addition of each ring, the observed heterogeneous OH uptake of cyclic compounds decreased by an additional 20 ± 8%. This unexpected result is in relative agreement with previous observations of a 30% difference in the relative rates of hopanes and steranes,[14] whose structures differ by the presence of one ring. The values shown in Figure 5b were calculated from total integrated signal of each compound class at each carbon number, composed almost entirely of branched isomers. An increase in relative oxidation rate from branching in cyclic hydrocarbons analogous to that observed in alkane isomers has been observed in the specific case of cholestane and androstane,[14] but isomers were not sufficiently resolved in higher N_{DBE} classes to provide this level of detail.

The mechanisms for the observed dependence of relative rates on cyclization and branching remain poorly understood and should be an area of focus for future studies, especially on the importance of this effect under atmospherically relevant conditions and gas-phase oxidation. Physical factors such as multiphase particles and differences in diffusion rates are not thought to account for differences in relative rates because time scales of diffusion (estimated for alkanes from Vardag et al.[35]) are expected to be several orders of magnitude faster than reactive OH uptake and good log−linear decay of all isomers supports the assumption of a well-mixed particle. Observed differences in reaction rates between structural isomers are therefore thought to be due at least in part to previously unstudied chemical mechanisms.

3.3. Overall OH Uptake by Hydrocarbon Mass. Relative rates measured here agreed with the small number of previously published results[6,14] but this work represents a much more comprehensive analysis of OH uptake by chemically reduced hydrocarbons in complex particles. Combining measured relative OH uptake coefficients with compositional analysis using eq 4, the overall uptake coefficient, γ_{eff}^{tot}, of the hydrocarbon mass in the particles was calculated to equal 0.86 ± 0.08, suggesting efficient OH uptake by unreacted hydrocarbons. This value was calculated with an initial composition, so represents an initial uptake coefficient that is in agreement with previous work on a compositionally similar complex hydrocarbon mixture.[10] However, differences in relative rates are expected to change the composition of the hydrocarbon mixture with time, so a more accurate value for average OH uptake by the hydrocarbon mixture can be calculated by measuring decay of the total hydrocarbon mixture. This direct measurement technique yielded a value of 0.72 ± 0.06. As the particulate matter becomes enhanced in cyclic compounds the overall reaction rate of hydrocarbons decreases, so the average uptake coefficient is expected to be lower than the initial uptake coefficient, as observed.

OH uptake is not equally efficient across structural classes, so the products of OH oxidation cannot be estimated solely from compositional analysis. Instead, the contribution of each compound class to the overall OH uptake can be determined

as shown in Figure 5c. Compounds that react more efficiently with OH account for a larger fraction of total OH uptake than the mass fraction would predict, such that branched alkanes account for approximately 20% of the mass of the particles, but ~33% of all OH uptake. An additional ~33% of hydroxyl radicals are expected to react with cycloalkanes, while the final third react with polycyclic aliphatic hydrocarbons. These fractions are of course dependent on particle source composition but are a reasonable estimate for the oxidation of hydrocarbon mass in atmospheric particles and highlight the importance in understanding relative OH uptake.

4. ATMOSPHERIC IMPLICATIONS

Heterogeneous oxidation rates of hydrocarbons in motor oil particles by hydroxyl radicals were observed in this work to be structurally dependent. While this has been demonstrated in previous work to be important for tracer method source attribution, it also has important implications for oxidation chemistry and aerosol transformations. Because branched alkanes are found to react 44 ± 14% faster than *n*-alkanes of the same carbon number (~30% faster when correcting for differences in volatility), the ratios of branched to straight alkanes are expected to change with atmospheric oxidation. Furthermore, particles are expected to become enhanced in cyclic compounds with atmospheric oxidation due to the observed 20 ± 8% decrease in oxidation rate with the addition of each ring. Consequently, the initial heterogeneous OH uptake by hydrocarbons in particles is dominated by less cyclic and more branched compounds and the composition is a function of photochemical age, with aged aerosols expected to be enhanced in polycyclic and straight-chain hydrocarbons. However, to fully constrain these compositional transformations, experiments under more atmospherically relevant conditions and analyses of the structural dependence of gas-phase reaction rates are necessary, as relevant properties of ambient aerosols or gases may differ from motor oil particles.

The application of GC × MS to oxidized motor oil yields new tools for studying ambient aerosol, alleviating the need to rely on only a few low-abundance well-resolved tracers. Newly accessible compounds provide a unique opportunity to use the composition of hydrocarbon particles as a photochemical clock, in which the ratio of compounds such as straight and branched or cyclic alkanes can be used to infer photochemical age. In contrast to most widely accepted gas-phase tracers of photochemical age (i.e., benzene and toluene as in ref 36), compounds studied in this work are semivolatile in the atmosphere, partitioning between gas and particle phase, and thus provide a means for measuring oxidation in mixed-phase or heterogeneous environments, assuming reliable knowledge about the composition of the initial particle.

The selective depletion of branched and relatively less-cyclic compounds affects not just oxidation rates, but also the expected products and pathways. Because tertiary carbon atoms have unique chemical pathways upon oxidation that can lead to decomposition, branching is expected to increase fragmentation into more volatile products upon oxidation, leading to loss of aerosol mass.[2] Alternately, cyclization, which slows reaction rates, provides fragmentation sites but also yields less volatile functionalized products due to ring-opening. The reaction products of the highly cyclic compounds measured in this work are not well-studied, but previous work has shown increased oxygen-to-carbon ratios in aerosol from a tricyclic precursor relative to acyclic precursors.[37] Shifts toward cyclic products with aerosol age will therefore affect oxidation products, pathways, and properties, though the details of these transformations and the influence of gas-phase processes remain understudied. While multiple generations of oxidation increase fragmentation of the oxidized products,[37] the inverse is true for the transition from unreacted hydrocarbons to lightly oxidized compounds. Enhancement of cyclization with photochemical age increases the importance of ring-opening functionalization pathways in the oxidation of hydrocarbons in aged particulate matter.

In areas downwind of major urban centers or subjected to significant anthropogenic influence, the hydrocarbon fraction of the aerosols will have a different chemical composition and different reaction products than freshly emitted particulate matter owing to the structural dependence of oxidation mechanisms. Buried in the previously unresolved complex mixtures in these ambient aerosols is information about sources and photochemical age. Though these applications are complicated by the presence of nonpetroleum-based hydrocarbon mixtures, future analyses of ambient environments can provide a basis for understanding source profiles. Improved understanding of the fates of branched and cyclic hydrocarbons is necessary to further constrain the fate of atmospheric aerosols, as they comprise a large fraction of the observed mass but are poorly resolved in current inventories.

■ ASSOCIATED CONTENT

Ⓢ Supporting Information

Supporting Information includes additional informations as noted in the text including Figures S-1−S-3 and eqs S-1−S-3. This material is available free of charge via the Internet at http://pubs.acs.org.

■ AUTHOR INFORMATION

Corresponding Author

*E-mail: gabriel.isaacman@berkeley.edu.

Notes

The authors declare no competing financial interest.

■ ACKNOWLEDGMENTS

We thank Kathryn R. Kolesar for assistance operating the flow tube reactor. The Advanced Light Source as well as KRW and TN are supported by the Director, Office of Energy Research, Office of Basic Energy Sciences, of the U.S. Department of Energy under Contract No. DE-AC02-05CH11231. CRR, AHG, and KRW are supported in part by the Laboratory Directed Research and Development Program of Lawrence Berkeley National Laboratory. Contributions by UCB personnel were supported in part by the National Oceanic and Atmospheric Administration award No. NA10OAR4310104. G.I. was funded by the U.S. Environmental Protection Agency (EPA) Science to Achieve Results (STAR) program, Fellowship Assistance Agreement No. FP-91781901-0. This work has not been formally reviewed by EPA. The views expressed in this work are solely those of the authors, and EPA does not endorse any products or commercial services mentioned.

■ REFERENCES

(1) Zhang, Q.; Jimenez, J. L.; Canagaratna, M. R.; Allan, J. D.; Coe, H.; Ulbrich, I. M.; Alfarra, M. R.; Takami, A.; Middlebrook, A. M.; Sun, Y. L.; Dzepina, K.; Dunlea, E. J.; Docherty, K. S.; DeCarlo, P. F.; Salcedo, D.; Onasch, T. B.; Jayne, J. T.; Miyoshi, T.; Shimono, A.; Hatakeyama, S.; Takegawa, N.; Kondo, Y.; Schneider, J.; Drewnick, F.;

Borrmann, S.; Weimer, S.; Demerjian, K.; Williams, P.; Bower, K.; Bahreini, R.; Cottrell, L.; Griffin, R. J.; Rautiainen, J.; Sun, J. Y.; Zhang, Y. M.; Worsnop, D. R. Ubiquity and dominance of oxygenated species in organic aerosols in anthropogenically-influenced Northern Hemisphere midlatitudes. *Geophys. Res. Let.* **2007**, *34*, 1−6.

(2) Kessler, S. H.; Smith, J. D.; Che, D. L.; Worsnop, D. R.; Wilson, K. R.; Kroll, J. H. Chemical sinks of organic aerosol: Kinetics and products of the heterogeneous oxidation of erythritol and levoglucosan. *Environ. Sci. Technol.* **2010**, *44*, 7005−7010.

(3) Smith, J. D.; Kroll, J. H.; Cappa, C. D.; Che, D. L.; Liu, C. L.; Ahmed, M.; Leone, S. R.; Worsnop, D. R.; Wilson, K. R. The heterogeneous reaction of hydroxyl radicals with sub-micron squalane particles: A model system for understanding the oxidative aging of ambient aerosols. *Atmos. Chem. Phys.* **2009**, *9*, 3209−3222.

(4) George, I. J.; Vlasenko, A.; Slowik, J. G.; Broekhuizen, K.; Abbatt, J. P. D. Heterogeneous oxidation of saturated organic aerosols by hydroxyl radicals: Uptake kinetics, condensed-phase products, and particle size change. *Atmos. Chem. Phys.* **2007**, *7*, 4187−4201.

(5) Che, D. L.; Smith, J. D.; Leone, S. R.; Ahmed, M.; Wilson, K. R. Quantifying the reactive uptake of OH by organic aerosols in a continuous flow stirred tank reactor. *Phys. Chem. Chem. Phys.* **2009**, *11*, 7885−7895.

(6) Lambe, A. T.; Miracolo, M. A.; Hennigan, C. J.; Robinson, A. L.; Donahue, N. M. Effective rate constants and uptake organic molecular markers in motor oil and diesel primary radicals. *Environ. Sci. Technol.* **2009**, *43*, 8794−8800.

(7) Hearn, J. D.; Smith, G. D. A mixed-phase relative rates technique for measuring aerosol reaction kinetics. *Geophys. Res. Let.* **2006**, *33*, 1−5.

(8) Bertram, A. K.; Ivanov, A. V.; Hunter, M.; Molina, L. T.; Molina, M. J. The Reaction Probability of OH on Organic Surfaces of Tropospheric Interest. *J. Phys. Chem. A* **2001**, *105*, 9415−9421.

(9) McNeill, V. F.; Yatavelli, R. L. N.; Thornton, J. A.; Stipe, C. B.; Landgrebe, O. Heterogeneous OH oxidation of palmitic acid in single component and internally mixed aerosol particles: Vaporization and the role of particle phase. *Atmos. Chem. Phys.* **2008**, *8*, 5465−5476.

(10) Kroll, J. H.; Smith, J. D.; Worsnop, D. R.; Wilson, K. R. Characterisation of lightly oxidised organic aerosol formed from the photochemical aging of diesel exhaust particles. *Environ. Chem.* **2012**, *9*, 211−220.

(11) Donahue, N. M.; Robinson, A. L.; Huff Hartz, K. E.; Sage, A. M.; Weitkamp, E. A. Competitive oxidation in atmospheric aerosols: The case for relative kinetics. *Geophys. Res. Let.* **2005**, *32*, 1−5.

(12) Huff Hartz, K. E.; Weitkamp, E. A.; Sage, A. M.; Donahue, N. M.; Robinson, A. L. Laboratory measurements of the oxidation kinetics of organic aerosol mixtures using a relative rate constants approach. *J. Geophys. Res.* **2007**, *112*, 1−13.

(13) Miracolo, M. A.; Presto, A. A.; Lambe, A. T.; Hennigan, C. J.; Donahue, N. M.; Kroll, J. H.; Worsnop, D. R.; Robinson, A. L. Photo-oxidation of low-volatility organics found in motor vehicle emissions: Production and chemical evolution of organic aerosol mass. *Environ. Sci. Technol.* **2010**, *44*, 1638−1643.

(14) Weitkamp, E. A.; Lambe, A. T.; Donahue, N. M.; Robinson, A. L. Laboratory Measurements of the Heterogeneous oxidation of condensed-phase organic molecular makers for motor vehicle exhaust. *Environ. Sci. Technol.* **2008**, *42*, 7950−7956.

(15) Goldstein, A. H.; Galbally, I. Known and unexplored organic constituents in the earth's atmosphere. *Environ. Sci. Technol.* **2007**, *41*, 1514−1521.

(16) Sieck, L. W. Determination of Molecular weight distribution of aromatic components in petroleum products by chemical ionization mass spectrometry with chlorobenzene as reagent gas. *Anal. Chem.* **1983**, *55*, 38−41.

(17) Isaacman, G.; Wilson, K. R.; Chan, A. W. H.; Worton, D. R.; Kimmel, J. R.; Nah, T.; Hohaus, T.; Gonin, M.; Kroll, J. H.; Worsnop, D. R.; Goldstein, A. H. Improved resolution of hydrocarbon structures and constitutional isomers in complex mixtures using gas chromatography-vacuum ultraviolet-mass spectrometry. *Anal. Chem.* **2012**, *84*, 2335−2342.

(18) Zimmermann, R.; Mühlberger, F.; Fuhrer, K.; Gonin, M.; Welthagen, W. An ultracompact photo-ionization time-of-flight mass spectrometer with a novel vacuum ultraviolet light source for on-line detection of organic trace compounds and as a detector for gas chromatography. *J. Mater Cycles Waste Manage.* **2008**, *10*, 24−31.

(19) Adam, T.; Zimmermann, R. Determination of single photon ionization cross sections for quantitative analysis of complex organic mixtures. *Anal. Bioanal. Chem.* **2007**, *389*, 1941−1951.

(20) Hanley, L.; Zimmermann, R. Light and molecular ions: The emergence of vacuum UV single-photon ionization in MS. *Anal. Chem.* **2009**, 4174−4182.

(21) Heimann, P. A.; Koike, M.; Hsu, C. W.; Blank, D.; Yang, X. M.; Suits, A. G.; Lee, Y. T.; Evans, M.; Ng, C. Y.; Flaim, C.; Padmore, H. A. Performance of the vacuum ultraviolet high-resolution and high-flux beamline for chemical dynamics studies at the advanced light source. *Rev. Sci. Instrum.* **1997**, *68*, 1945−1951.

(22) Eschner, M. S.; Welthagen, W.; Gröger, T. M.; Gonin, M.; Fuhrer, K.; Zimmermann, R. Comprehensive multidimensional separation methods by hyphenation of single-photon ionization time-of-flight mass spectrometry (SPI-TOF-MS) with GC and GCxGC. *Anal. Bioanal. Chem.* **2010**, *398*, 1435−1445.

(23) Geissler, R.; Saraji-bozorgzad, M. R.; Gro, T.; Fendt, A.; Streibel, T.; Sklorz, M.; Krooss, B. M.; Fuhrer, K.; Gonin, M.; Kaisersberger, E.; Denner, T.; Zimmermann, R. Single photon ionization orthogonal acceleration time-of-flight mass spectrometry and resonance enhanced multiphoton ionization time-of-flight mass spectrometry for evolved gas analysis in thermogravimetry: Comparative analysis of crude oils. *Anal. Chem.* **2009**, *81*, 6038−6048.

(24) Kroll, J. H.; Smith, J. D.; Che, D. L.; Kessler, S. H.; Worsnop, D. R.; Wilson, K. R. Measurement of fragmentation and functionalization pathways in the heterogeneous oxidation of oxidized organic aerosol. *Phys. Chem. Chem. Phys.* **2009**, *11*, 8005−8014.

(25) Atkinson, R. Kinetics of the gas-phase reactions of OH radicals with alkanes and cycloalkanes. *Atmos. Chem. Phys.* **2003**, *3*, 4183−4358.

(26) Renbaum, L. H.; Smith, G. D. Artifacts in measuring aerosol uptake kinetics: The roles of time, concentration and adsorption. *Atmos. Chem. Phys.* **2011**, *11*, 6881−6893.

(27) Mao, D.; Weghe, H. V. D.; Lookman, R.; Vanermen, G.; Brucker, N. D.; Diels, L. Resolving the unresolved complex mixture in motor oils using high-performance liquid chromatography followed by comprehensive two-dimensional gas chromatography. *Fuel.* **2009**, *88*, 312−318.

(28) Gentner, D. R.; Isaacman, G.; Worton, D. R.; Chan, A. W. H.; Dallmann, T. R.; Davis, L.; Liu, S.; Day, D. A.; Russell, L. M.; Wilson, K. R.; Weber, R.; Guha, A.; Harley, R. A.; Goldstein, A. H. Elucidating secondary organic aerosol from diesel and gasoline vehicles through detailed characterization of organic carbon emissions (submitted).

(29) DeCarlo, P. F.; Kimmel, J. R.; Trimborn, A.; Northway, M. J.; Jayne, J. T.; Aiken, A. C.; Gonin, M.; Fuhrer, K.; Horvath, T.; Docherty, K. S.; Worsnop, D. R.; Jimenez, J. L. Field-deployable, high-resolution, Time-of-flight aerosol mass spectrometer. *Anal. Chem.* **2006**, *78*, 8281−8289.

(30) Sueper, D. ToF-AMS Analysis Software 2012. http://cires.colorado.edu/jimenez-group/wiki/index.php/ToF-AMS_Analysis_Software (accessed June 27, 2012).

(31) Williams, B. J.; Goldstein, A. H.; Kreisberg, N. M.; Hering, S. V.; Worsnop, D. R.; Ulbrich, I. M.; Docherty, K. S.; Jimenez, J. L. Major components of atmospheric organic aerosol in southern California as determined by hourly measurements of source marker compounds. *Atmos. Chem. Phys.* **2010**, *10*, 11577−11603.

(32) Kroll, J. H.; Seinfeld, J. H. Chemistry of secondary organic aerosol: Formation and evolution of low-volatility organics in the atmosphere. *Atmos. Environ.* **2008**, *42*, 3593−3624.

(33) Isaacman, G.; Worton, D. R.; Kreisberg, N. M.; Hennigan, C. J.; Teng, a. P.; Hering, S. V.; Robinson, A. L.; Donahue, N. M.; Goldstein, A. H. Understanding evolution of product composition and volatility distribution through in-situ GCxGC analysis: A case study of longifolene ozonolysis. *Atmos. Chem. Phys.* **2011**, *11*, 5335−5346.

(34) Kwok, E. S. C.; Atkinson, R. Estimation of hydroxyl radical reaction rate constants for gas-phase organic compounds using a structure-reactivity relationship: An update. *Atmos. Environ.* **1995**, *29*, 1685−1695.
(35) Vardag, T.; Karger, N.; Ludemann, H.-D. Temperature and pressure dependence of self diffusion in long liquid *n*-alkanes. *Ber. Bunsen-Ges. Phys. Chemie.* **1991**, *95*, 859−865.
(36) de Gouw, J. A.; Middlebrook, A. M.; Warneke, C.; Goldan, P. D.; Kuster, W. C.; Roberts, J. M.; Fehsenfeld, F. C.; Worsnop, D. R.; Canagaratna, M. R.; Pszenny, A. A. P.; Keene, W. C.; Marchewka, M.; Bertman, S. B.; Bates, T. S. Budget of organic carbon in a polluted atmosphere: Results from the New England Air Quality Study in 2002. *J. Geophys. Res.* **2005**, *110*, 1−22.
(37) Lambe, A. T.; Onasch, T. B.; Croasdale, D. R.; Wright, J. P.; Martin, A. T.; Franklin, J. P.; Massoli, P.; Kroll, J. H.; Canagaratna, M. R.; Brune, W. H.; Worsnop, D. R.; Davidovits, P. Transitions from functionalization to fragmentation reactions of laboratory secondary organic aerosol (SOA) generated from the OH oxidation of alkane precursors. *Environ. Sci. Technol.* **2012**, *46*, 5430−5437.